

Elastic and Inelastic Scattering of Fast Neutrons from Co, Cu, and Zn†

A. B. SMITH, C. A. ENGELBRECHT,* AND D. REITMANN*

Argonne National Laboratory, Argonne, Illinois

(Received 20 February 1964)

Cross sections and angular distributions were measured for the elastic and the inelastic scattering of neutrons from natural Co, Cu, and Zn in the energy range 300 keV to 1.5 MeV. The measured values are compared with the results of optical-model calculations using spin assignments which are either known or consistent with shell-model predictions. The effect of resonance width fluctuations is investigated. The theoretically calculated elastic scattering angular distributions are in good agreement with the experimental cross sections. Theoretical consideration of resonance width fluctuations tends to result in better agreement with the measured Cu inelastic cross sections.

INTRODUCTION

A NUMBER of studies of fast-neutron scattering from Co, Cu, and Zn have been reported.¹⁻⁸ At incident neutron energies above the thresholds for inelastic scattering, however, the methods employed in these studies have often failed to separate the elastic and the inelastic processes. Studies of inelastic neutron scattering have largely been confined to incident neutron energies above several MeV or have consisted of indirect studies of the gamma-ray emission following inelastic scattering.⁹⁻¹² The latter method is particularly useful near the reaction thresholds but is troubled with normalization and resolution problems and with uncertainties in the respective gamma-ray transitions.

This direct study of elastic and of inelastic scattering from Cu, Co, and Zn was undertaken with the objective of providing experimental knowledge suitable for definitive theoretical interpretations based upon the optical model. It was also desirable to obtain this basic neutron information for use in macroscopic applied work.

EXPERIMENTAL METHOD AND RESULTS

The pulsed-beam fast time-of-flight technique was utilized to achieve the necessary experimental velocity

† This work supported by the U. S. Atomic Energy Commission.

* Present address: South African Atomic Energy Board, Pretoria, Republic of South Africa.

¹ R. O. Lane, A. S. Langsdorf, Jr., J. E. Monahan, and A. J. Elwyn, *Ann. Phys. (N. Y.)* **12**, 135 (1961); see also Argonne National Laboratory Report ANL-5567, 1956 (unpublished).

² S. A. Cox, *Bull. Am. Phys. Soc.* **8**, 478 (1963).

³ M. Walt and H. Barschall, *Phys. Rev.* **93**, 1062 (1954).

⁴ D. Reitmann and A. Smith, *Bull. Am. Phys. Soc.* **7**, 334 (1962).

⁵ S. E. Darden, R. B. Perkins, and R. B. Walton, *Phys. Rev.* **100**, 1315 (1955).

⁶ Y. A. Aleksandrov, G. V. Anikin, and A. S. Soldatov, *Zh. Eksperim. i Teor. Fiz.* **40**, 1878 (1961) [English transl.: *Soviet Phys.—JETP* **13**, 1319 (1961)].

⁷ K. Tsukada, S. Tanaka, M. Maruyama, and Y. Tomita, *Phys. Fast Intermediate Reactors, Vienna* **1**, 75 (1962).

⁸ See for review: Brookhaven National Laboratory Report-BNL-400, edited by M. D. Goldberg, V. M. May, and J. R. Stehn, 1962 (unpublished), 2nd ed., Vol. II.

⁹ R. B. Day, *Phys. Rev.* **102**, 767 (1956).

¹⁰ L. Cranberg and J. S. Levin, *Phys. Rev.* **103**, 343 (1956).

¹¹ W. E. Meyerhof (private communication).

¹² T. Wiedling (private communication).

resolution. A pulsed Van de Graaff machine was coupled to a magnetic bunching system to provide proton bursts of ~ 1 -nsec duration at duty cycles of 0.3 to 1.5%. The subsequent neutron bursts were derived from the $\text{Li}^7(p,n)\text{Be}^7$ reaction in metal targets 15 to 30 keV thick. The scattering samples were right cylinders 1.78 cm long and 1.78 cm in diameter suspended approximately 10 cm from the target. Neutrons scattered from these samples were timed over flight paths of 1 to 2 m. A detailed description of the experimental method and apparatus is given elsewhere.¹³

The time spectra of elastically scattered neutrons were measured at ten or more angles between 20 and 145 deg. The measurements were made at incident neutron energy intervals of ~ 50 keV from 0.3 to 1.5 MeV. A representative experimental time spectrum is shown in Fig. 1. The elastic components, the inelastic groups, and the gamma rays originating in the source and the sample are resolved. The measured intensities of the neutron groups were corrected for the attenuation of the incident beam and for multiple scattering

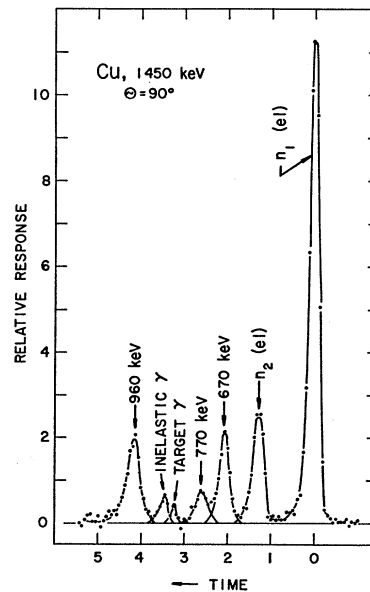


FIG. 1. An experimental time spectrum obtained by scattering 1450-keV neutrons from natural copper. Elastic scattering of the two neutron groups from the $\text{Li}^7(p,n)\text{Be}^7$ source is evident. Inelastic groups resulting in the excitation of 970-, 670-, and 770-keV levels are resolved.

¹³ A. B. Smith, *Z. Physik* **175**, 242 (1963).

within the sample, using a Monte Carlo procedure described elsewhere.¹⁸ All measured cross sections were normalized to the known differential elastic scattering cross section of carbon and were expressed as cross sections of the natural element.¹

The measured differential elastic scattering cross sections of Cu, Co, and Zn were fitted, by the method of least squares, with a series of Legendre polynomials of the form

$$\frac{d\sigma}{d\Omega} = \frac{\sigma}{4\pi} \left[1 + \sum_{i=1}^4 \omega_i P_i \right], \quad (1)$$

where P_i is the Legendre polynomial, and ω_i and σ are derived from the fit to the experimental data. The measured elastic scattering cross sections, expressed in the form of Eq. (1), are given in Fig. 2 and Tables I(a), (b), and (c). The errors pertaining to the coefficients ω_i are standard deviations derived from the least-square fitting procedure. As such, they represent the "goodness" of the fit of Eq. (1) to the actual experimental results. The uncertainties in the σ values are estimated to be 5 to 8% including the error in the cross section of the carbon standard.

TABLE I. Elastic scattering from Cu, Zn, and Co expressed in the form of Eq. (1).

E_n (MeV)	σ (el) (b)	ω_1	ω_2	ω_3	ω_4
(a) Cu					
0.30	5.56	0.234±0.020	0.110±0.034	0.076±0.038	0.087±0.050
0.34	4.64	0.412±0.011	0.214±0.019	0.097±0.021	0.032±0.027
0.39	4.52	0.396±0.018	0.221±0.031	0.064±0.035	0.034±0.046
0.44	4.66	0.284±0.016	0.184±0.027	0.063±0.032	-0.007±0.038
0.49	4.65	0.360±0.011	0.192±0.019	0.045±0.021	0.006±0.026
0.55	4.55	0.365±0.012	0.309±0.021	0.032±0.025	0.089±0.031
0.59	4.54	0.402±0.008	0.315±0.015	0.082±0.017	0.039±0.021
0.64	3.95	0.471±0.042	0.395±0.071	0.113±0.084	0.042±0.108
0.69	3.90	0.496±0.028	0.375±0.048	0.116±0.055	0.041±0.071
0.74	3.78	0.389±0.033	0.330±0.056	0.027±0.067	0.034±0.086
0.79	3.93	0.439±0.017	0.405±0.026	0.096±0.036	0.052±0.043
0.84	3.74	0.515±0.021	0.541±0.035	0.103±0.041	0.042±0.053
0.88	4.24	0.449±0.029	0.401±0.043	0.193±0.056	0.055±0.061
0.93	3.48	0.588±0.043	0.470±0.063	0.225±0.083	-0.058±0.091
0.98	3.95	0.473±0.031	0.544±0.048	0.143±0.075	0.283±0.098
0.99	3.36	0.465±0.033	0.625±0.055	0.311±0.066	0.071±0.084
1.04	3.09	0.559±0.016	0.614±0.026	0.242±0.031	0.038±0.040
1.09	2.91	0.603±0.026	0.704±0.045	0.350±0.052	0.117±0.067
1.14	2.97	0.533±0.010	0.755±0.017	0.342±0.020	0.119±0.026
1.19	2.51	0.633±0.039	0.700±0.066	0.394±0.078	0.216±0.093
1.25	2.88	0.575±0.052	0.734±0.076	0.394±0.099	0.246±0.111
1.30	2.85	0.651±0.051	0.976±0.080	0.540±0.101	0.418±0.129
1.35	2.63	0.597±0.038	1.055±0.057	0.448±0.076	0.433±0.085
1.40	2.60	0.702±0.019	1.035±0.027	0.517±0.036	0.281±0.040
1.45	2.45	0.708±0.034	0.999±0.051	0.616±0.067	0.395±0.075
1.50	2.41	0.737±0.037	1.083±0.052	0.598±0.070	0.461±0.077
(b) Zn					
0.30	5.55	0.315±0.022	0.210±0.037	0.051±0.043	0.059±0.055
0.34	5.00	0.384±0.036	0.276±0.062	0.048±0.070	0.007±0.091
0.39	4.96	0.447±0.027	0.338±0.047	0.051±0.053	0.123±0.069
0.44	5.10	0.374±0.023	0.212±0.039	0.076±0.046	-0.103±0.055
0.49	5.14	0.390±0.014	0.261±0.024	0.074±0.027	0.029±0.033
0.55	4.69	0.375±0.010	0.358±0.017	0.042±0.020	0.091±0.026
0.59	4.74	0.451±0.008	0.351±0.013	0.069±0.015	0.091±0.019
0.64	4.25	0.435±0.042	0.448±0.070	0.066±0.084	0.111±0.108
0.69	4.14	0.509±0.020	0.472±0.034	0.070±0.038	0.131±0.050
0.74	3.77	0.403±0.057	0.425±0.097	0.067±0.115	0.050±0.148
0.79	4.27	0.526±0.035	0.474±0.058	0.096±0.068	0.004±0.083
0.84	3.72	0.497±0.012	0.490±0.020	0.123±0.023	0.047±0.030
0.88	4.37	0.442±0.021	0.436±0.032	0.139±0.041	0.040±0.045
0.93	3.93	0.583±0.020	0.455±0.030	0.141±0.039	0.032±0.044
0.98	4.01	0.481±0.019	0.577±0.029	0.198±0.038	0.157±0.049
0.99	3.77	0.561±0.014	0.682±0.024	0.200±0.028	0.078±0.039
1.04	3.22	0.556±0.023	0.709±0.039	0.182±0.044	0.144±0.057
1.09	3.10	0.494±0.058	0.779±0.102	0.256±0.114	0.143±0.146
1.14	3.25	0.551±0.019	0.677±0.034	0.188±0.038	0.075±0.048
1.19	2.67	0.630±0.029	0.948±0.048	0.315±0.057	0.242±0.068
1.25	2.95	0.627±0.036	0.854±0.052	0.343±0.069	0.269±0.077
1.30	2.76	0.823±0.006	1.010±0.009	0.487±0.011	0.048±0.014
1.35	2.88	0.711±0.040	1.050±0.060	0.418±0.079	0.409±0.089
1.40	2.51	0.765±0.030	0.895±0.043	0.452±0.057	0.132±0.064
1.45	2.64	0.745±0.040	1.081±0.058	0.582±0.077	0.408±0.086
1.50	2.63	0.845±0.018	1.103±0.027	0.614±0.035	0.362±0.040

TABLE I (continued)

E_n (MeV)	σ (el) (b)	ω_1	ω_2	ω_3	ω_4
(c) Co					
0.30	5.03	0.293±0.013	0.110±0.020	-0.004±0.026	-0.012±0.029
0.35	4.16	0.196±0.035	0.244±0.051	0.082±0.067	0.084±0.075
0.40	3.91	0.343±0.008	0.146±0.011	0.028±0.015	0.022±0.017
0.45	4.45	0.271±0.027	0.272±0.040	-0.028±0.052	0.079±0.059
0.50	4.88	0.278±0.020	0.215±0.029	0.089±0.037	-0.008±0.042
0.55	3.65	0.400±0.023	0.308±0.033	0.015±0.044	0.117±0.049
0.60	4.11	0.355±0.010	0.331±0.015	0.123±0.020	0.039±0.022
0.65	4.12	0.378±0.021	0.488±0.031	0.119±0.040	0.062±0.045
0.70	4.27	0.360±0.015	0.440±0.021	0.107±0.028	0.012±0.031
0.75	3.66	0.501±0.036	0.511±0.052	0.110±0.069	-0.025±0.077
0.80	3.47	0.406±0.018	0.532±0.038	0.126±0.039	-0.053±0.042
0.85	3.47	0.320±0.016	0.729±0.024	0.027±0.031	0.245±0.035
0.90	3.15	0.351±0.018	0.664±0.026	0.163±0.034	0.024±0.038
0.95	3.68	0.446±0.015	0.709±0.027	0.224±0.040	0.106±0.041
1.00	2.94	0.422±0.041	0.793±0.059	0.279±0.078	0.185±0.087
1.05	3.36	0.440±0.027	0.845±0.039	0.213±0.052	0.144±0.058
1.10	3.05	0.582±0.021	0.749±0.030	0.196±0.040	0.076±0.045
1.15	3.30	0.418±0.030	0.779±0.044	0.333±0.058	0.159±0.065
1.20	3.36	0.525±0.025	0.841±0.041	0.363±0.054	0.178±0.060
1.25	3.30	0.584±0.020	0.904±0.030	0.403±0.039	0.160±0.044
1.30	3.18	0.632±0.026	1.076±0.038	0.509±0.049	0.278±0.055
1.35	2.84	0.562±0.017	0.940±0.025	0.484±0.034	0.160±0.038
1.40	2.75	0.669±0.024	1.047±0.035	0.529±0.046	0.258±0.051
1.45	2.89	0.580±0.040	1.027±0.059	0.498±0.077	0.248±0.086
1.50	2.65	0.762±0.016	1.162±0.024	0.620±0.031	0.290±0.035

It is evident in Fig. 2 that the measured elastic cross sections of Co, below an incident neutron energy of ~500 keV, vary considerably more than would be expected from the estimated error. In the case of Co, and to a lesser extent Cu and Zn, these variations are princi-

pally due to resonance effects. At incident energies of ~500 keV, the ~20-keV energy spread of neutrons leaving the source is not large compared to the resonance widths and spacings. Thus, the values of the Co cross section given in Fig. 2 are not a "good" average of

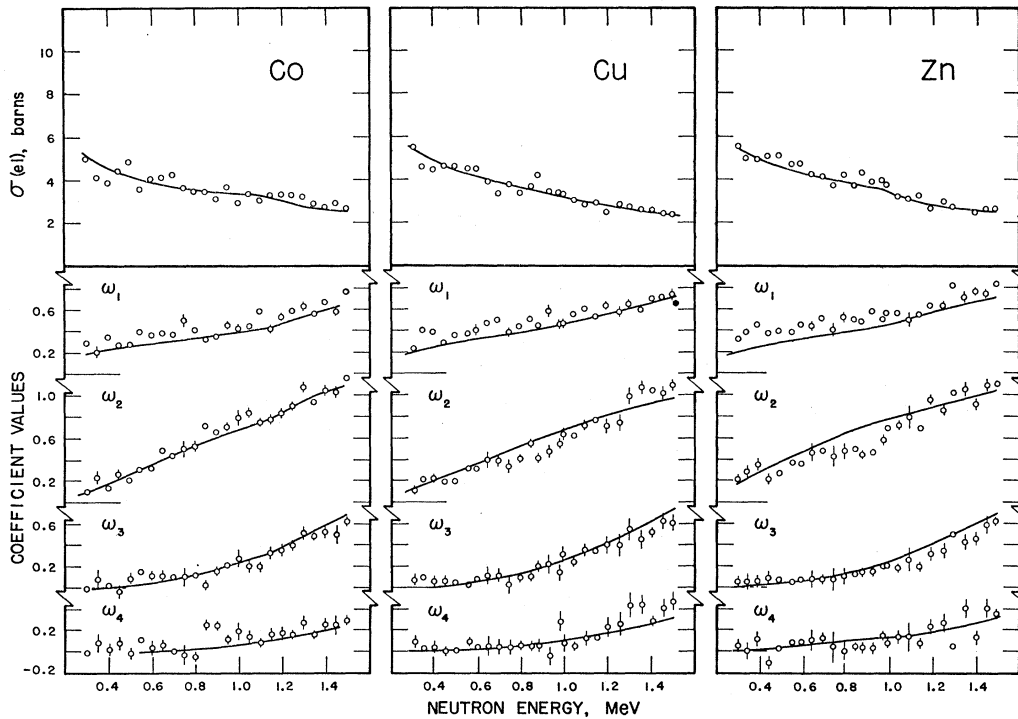


FIG. 2. Differential elastic scattering cross section of Co, Cu, and Zn expressed in the form of Eq. (1). Curves represent calculated values.

the resonance structure. This prominence of the resonance structure is evident in Fig. 3, which shows the total cross section of Co measured from 0.35 to 0.55 MeV with resolutions of 1.0 to 1.8 keV. These total cross-section measurements were made using pulsed beam techniques on a flight path of 25 m. The time of transit of the neutrons transmitted through the sample, over this flight path, was measured to precisely determine the neutron energy. Recent precision total cross-section measurements with Cu show a much smaller resonance effect¹⁴ than in the case of Co.

Below the inelastic thresholds, the elastic cross sections given in Fig. 2 and Table I are in good agreement with the total scattering angular distributions of Langsdorf *et al.*¹ When the latter results are corrected for the inelastic content, the agreement extends throughout the measured energy range. The results of this experiment are also in good agreement with those obtained by a number of workers studying elastic scattering at isolated incident energies and/or angles.^{3,5,8}

Four neutron groups resulting from inelastic scattering to levels in Cu at 670, 770, 960, and 1110 keV were observed. These levels correspond to the known¹⁵ 668- and 961-keV states in Cu⁶³ and the 770- and 1114-keV states in Cu⁶⁵. Scattering to the 670-, 770-, and 960-keV level was measured to be isotropic to within

TABLE II. Inelastic scattering from Cu, Zn, and Co.

E_n (MeV)	(a) Cu				
	$\sigma(0.67$ MeV) (b)	$\sigma(0.77$ MeV) (b)	$\sigma(0.96$ MeV) (b)	$\sigma(1.11$ MeV) (b)	
1.00	0.124 ± 0.030				
1.09	0.121 ± 0.020				
	0.151 ± 0.020				
1.10	0.139 ± 0.020				
	0.141 ± 0.020	0.029 ± 0.015			
1.14	0.097 ± 0.020	0.040 ± 0.015			
1.15	0.104 ± 0.020				
1.19	0.117 ± 0.020	0.057 ± 0.015			
	0.167 ± 0.020				
1.20	0.129 ± 0.015				
1.29	0.138 ± 0.015	0.090 ± 0.020	0.241 ± 0.060		
1.30		0.076 ± 0.020			
	0.136 ± 0.015	0.091 ± 0.020	0.131 ± 0.050		
1.35	0.136 ± 0.015	0.124 ± 0.025			
1.40	0.148 ± 0.030	0.070 ± 0.020	0.195 ± 0.040		
	0.133 ± 0.015	0.071 ± 0.020	0.200 ± 0.040		
			0.258 ± 0.030	< 0.145	
1.44	0.133 ± 0.020	0.076 ± 0.020	0.229 ± 0.030	0.118 ± 0.035	
1.45	0.137 ± 0.025	0.141 ± 0.025	0.209 ± 0.030		
1.50	0.138 ± 0.025	0.111 ± 0.020	0.206 ± 0.030		
	0.162 ± 0.025	0.121 ± 0.020	0.232 ± 0.030		
	0.183 ± 0.025	0.120 ± 0.020	0.300 ± 0.035	0.220 ± 0.040	

(b) Zn ^a		
E_n (MeV)	σ (sum of three levels) (b)	
1.40	0.760 ± 0.150	
1.45	0.690 ± 0.100	
1.50	0.760 ± 0.100	

(c) Co		
E_n (MeV)	$\sigma(1.068$ MeV) (b)	$\sigma(1.190$ MeV) (b)
1.45	0.082 ± 0.020	
1.50	0.140 ± 0.030	0.390 ± 0.110

^a Intensity ratio 990; 1040; 1080 keV = 1.72: 1.514: 1.0.

¹⁴ S. A. Cox (private communication).

¹⁵ *Nuclear Data Sheets* (National Academy of Sciences—National Research Council, Washington, D. C., 1960), NRC 60-5-58.

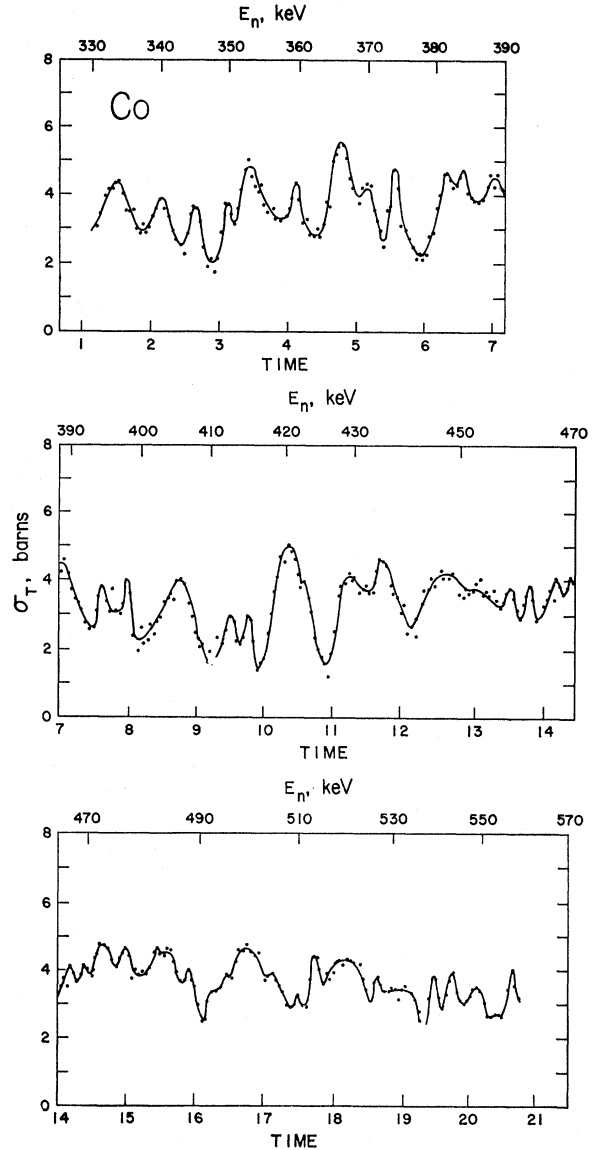


FIG. 3. Total cross section of Co from 330 to 550 keV.

~15%. Scattering to the 1110-keV level was determined at only one angle (90 deg) and was assumed isotropic. The measured cross sections for the excitation of these levels are given in Fig. 4 and Table II(a). All values refer to the natural element. The errors shown are estimates including uncertainties in the carbon standard cross section, the energy dependence of the detector sensitivity, and the statistical precision of the actual measurements. Each measurement was independently carried out and normalized. The results are in good agreement with the results of recent studies^{11,12} of gamma-ray emissions following inelastic neutron scattering from Cu.

The predominant isotopes of natural zinc are 64, 66, and 68. The first excited states are at 990, 1040, and 1080 keV, respectively. Inelastic scattering to each of

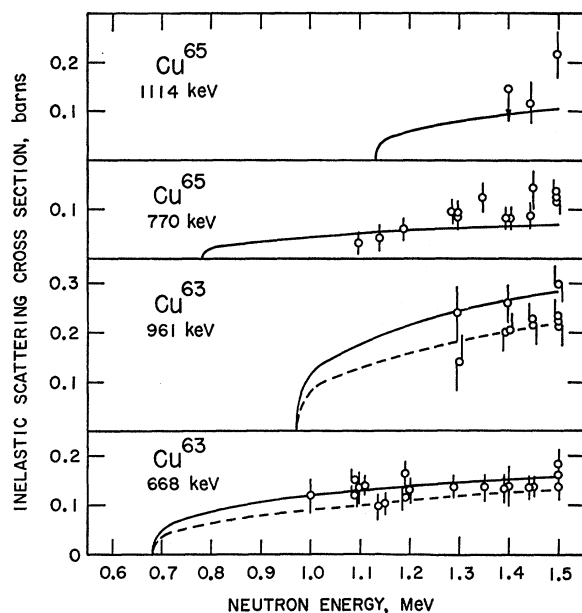


FIG. 4. Inelastic excitation cross sections of copper. Curves indicate calculated values (see text).

these states was observed with the respective relative intensities of 1.7, 1.5, and 1.0. These ratios are similar to the relative abundance of the isotopes of the natural element. The combined excitation of these three levels was found to be isotropic to within $\sim 25\%$. The measured inelastic cross sections for the combined excitation of the three levels are given in Table II(b) and Fig. 5(a). In Co, the intensity of inelastic neutron groups corresponding to the excitation of known levels at 1097 and at 1189 keV were measured. In each case the measurements were made at only one angle (90 deg). The angular distributions were assumed to be isotropic in deriving the integrated cross sections given in Table II(b) and Fig. 5(b).

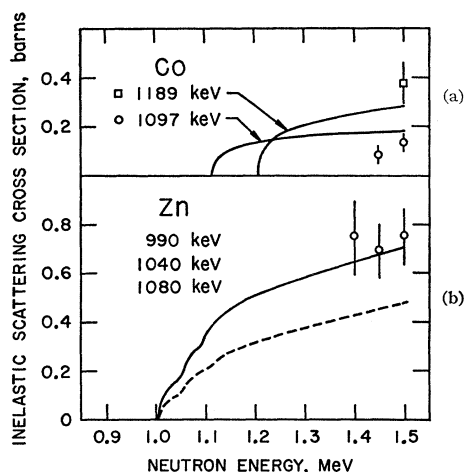


FIG. 5. Inelastic excitation cross sections of Co (a) and Zn (b). Curves indicate calculated values (see text).

DISCUSSION

Elastic Scattering

In the energy region under consideration, the dependence of the average total cross section on energy and on mass number can be described satisfactorily by means of a complex potential well which is spherically symmetric (for $40 \leq A \leq 150$) and has constant parameters, apart from the radius which is usually taken to vary with A as $R = r_0 A^{1/3} + r_1$. A commonly used potential shape is

$$-Vq(r) - iWp(r) + V_{s0} \left(\frac{\hbar}{\mu\pi c} \right)^2 \sigma \cdot \mathbf{l} \frac{1}{r} \frac{dq}{dr}, \quad (2)$$

with form factors

$$q(r) = \left[1 + \exp\left(\frac{r-R}{a} \right) \right]^{-1}, \quad (3)$$

and

$$p(r) = \exp\left[-\left(\frac{r-R-d}{b} \right)^2 \right].$$

A good fit to s -wave neutron strength functions, total cross sections, and elastic angular distributions (below inelastic thresholds) was recently obtained¹⁶ by means of the following set of parameters:

$$\begin{aligned} W &= 14 \text{ MeV} & b &= 0.50 \text{ F} & d &= 0.5 \text{ F} \\ V &= 46 \text{ MeV} & r_0 &= 1.16 \text{ F} & r_1 &= 0.6 \text{ F} \\ V_{s0} &= 7 \text{ MeV} & a &= 0.62 \text{ F}. \end{aligned} \quad (4)$$

The curves on Fig. 1 represent elastic scattering cross sections and angular distribution coefficients calculated using this parameter set. Above inelastic thresholds, the calculated values depend on the use of the Hauser-Feshbach approximation.¹⁷ All calculations of elastic cross sections and angular distributions were performed by means of the ABACUS-2 computer code.¹⁸

The parameters of Eq. (4), which were chosen to give the best over-all fit for $40 \leq A \leq 150$, actually yielded results which agree very well with the present experimental measurements. The largest disagreement occurs in ω_1 , for which the calculated values are perhaps slightly too small. If the parameter d is increased to 0.75 F, the values obtained for ω_1 are about 25% larger. At the same time, ω_3 is increased by about 15%, $\sigma(\text{el})$ by 8 or 9%, and ω_4 by 5%, while the inelastic cross sections are decreased slightly at low energies and increased slightly at high energies. The improvement in the ω_1 fit is considered too small to justify modification of the general set of parameters.

¹⁶ P. A. Moldauer, Nucl. Phys. **47**, 65 (1963).

¹⁷ W. Hauser and H. Feshbach, Phys. Rev. **87**, 366 (1952).

¹⁸ E. H. Auerbach, Brookhaven National Laboratory Report, BNL-6562 (revised version), 1962 (unpublished).

Inelastic Scattering

Since the optical model does not provide a way of determining the branching ratios between various decay modes of the compound nucleus, a more specific model is required for the discussion of inelastic scattering. A model which is widely used is the one developed by Hauser and Feshbach,¹⁷ according to which the cross section for the excitation of level b is given by

$$\sigma_{ab} = \pi\lambda^2 \sum_{\alpha\beta J} g_J (T_\alpha^J T_\beta^J / \sum_\gamma T_\gamma^J), \quad (5)$$

where α and β indicate the angular momenta (l, j) for the incident and outgoing neutrons, respectively, where J represents the angular momentum and parity of the compound nucleus, while \sum_γ implies a summation over all open channels.

This expression [Eq. (5)] should, however, be multiplied by a width fluctuation factor^{19,20} which depends on the distribution of level widths in the compound nucleus (a Porter-Thomas distribution²¹ has almost always been assumed for the neutron widths). A more careful averaging process applied to the R -matrix theory expressions for the cross sections has led to the conclusion^{20,22} that the transmission coefficients T which occur in Eq. (5) should, furthermore, be replaced by analogous quantities which under circumstances which apply to the cases considered here, have the form

$$\theta = T + 2(1-\phi)[1-(1-T)^{1/2}]^2, \quad (6)$$

where ϕ is a known function of the total width to spacing ratio and can have values ranging from 0 to 1. When these modifications are introduced, one finds that the inelastic cross sections reach their largest values when $\phi=0$. Calculations of inelastic scattering cross sections were carried out by means of the NEARREX computer code²³ for the Hauser-Feshbach case and with the inclusion of the width fluctuation correction and the modification of Eq. (6) (using $\phi=0$). The optical-model transmission coefficients were calculated by means of the ABACUS computer code.

The inelastic scattering calculations require a knowledge of the spins and parities of the initial and final nuclear states. The Co⁵⁹ ground-state spin of $7/2^-$ is easily understood in terms of a hole in the $1f_{7/2}$ proton shell, which is filled in nickel with $Z=28$. Similarly, the $3/2^-$ ground states of Cu⁶³ and Cu⁶⁵ are due to the addition of a $2p_{3/2}$ proton to the $Z=28$ closed shell. The positions of the single-particle excited states in these nuclei

can be estimated by making use of the average level spacings observed²⁴ in this mass number region. Thus, in cobalt, one could expect a $3/2^-$ state anywhere from 1.3 to 1.9 MeV and a $3/2^+$ state between 1.3 and 3.1 MeV. The $1f_{5/2}$ and $2p_{1/2}$ excitations in the copper isotopes can be expected to occur near 1 and 2 MeV, respectively.

Actually the lowest states of these nuclei are usually assumed to be due to a 2^+ excitation of the even-even core²⁵ rather than to single-particle excitations. If pure $j-j$ coupling is assumed, such an excitation gives rise to a group of levels whose center of gravity agrees with the excitation energy of the 2^+ level in the corresponding even nucleus. Thus, the 1097-keV ($5/2^-$) and 1289-keV ($3/2^-$) levels in Co⁵⁹ probably belong to such a group. In order to agree with the 1332-keV 2^+ level in Ni⁶⁰, the 1189-keV level in cobalt must have a spin value $7/2^-$ or $9/2^-$. The latter value was assumed for calculational purposes. Using $7/2^-$ instead would tend to reduce the cross sections for the excitation of any of the first three levels in cobalt.

Recent experimental measurements²⁶ on inelastically scattered protons and on gamma rays following Coulomb excitation of the copper isotopes indicate spins $1/2^-$ for the 668- and 770-keV levels (in Cu⁶³ and Cu⁶⁵, respectively), $5/2^-$ for the 961- and 1114-keV levels and $7/2^-$ for the 1327- and 1482-keV levels. If these levels are assumed to correspond to pure excited core states,²⁵ one is faced with the absence of the expected single particle $5/2^-$ state. It appears,²⁷ however, that the $1/2^-$ and $5/2^-$ levels contain about 30% admixtures of the single particle $p_{1/2}$ and $f_{5/2}$ states, as well as almost 20% admixtures of higher core excitations.

The results of the inelastic scattering calculation for the copper isotopes are shown in Fig. 4. For the 668- and 961-keV levels, the cross sections according to the Hauser-Feshbach theory are indicated by the solid curves while the dashed curves include the width fluctuation correction and modified transmission coefficients. The agreement with the experimental data points, although perhaps slightly better for the former, is good for both solid and dashed curves. For the Cu⁶⁵ levels, only the Hauser-Feshbach cross sections are shown. The calculated values are on the low side for both levels. The angular distribution of the inelastically scattered neutrons was also calculated for the 668-keV level. Even at a neutron energy of 1500 keV ω_2 [see Eq. (1)] is found to have a value of only 0.077. This difference of 7% between the 0-deg and 90-deg cross sections is smaller than the uncertainty in the measured values, which supports the observation of isotropy.

¹⁹ A. M. Lane and J. E. Lynn, Proc. Phys. Soc. (London) **A70**, 557 (1957). L. Dresner, Columbia University Report CU-175, 1957 (unpublished), p. 71.

²⁰ P. A. Moldauer, Phys. Rev. **123**, 968 (1961); Bull. Am. Phys. Soc. **7**, 334 (1962).

²¹ C. E. Porter and R. G. Thomas, Phys. Rev. **104**, 483 (1956).

²² P. A. Moldauer, 1963 (unpublished), and Phys. Rev. (to be published).

²³ P. A. Moldauer, C. A. Engelbrecht, and G. J. Duffy, Argonne National Laboratory Report, 1964 (unpublished).

²⁴ R. H. Nussbaum, Rev. Mod. Phys. **28**, 423 (1956).

²⁵ R. D. Lawson and J. L. Uretsky, Phys. Rev. **108**, 1300 (1957); A. de Shalit, *ibid.* **122**, 1530 (1961).

²⁶ R. L. Robinson, F. K. McGowan, and P. H. Stelson, Oak Ridge National Laboratory Report, ORNL-3425, 1963 (unpublished), p. 22; F. Perey, R. J. Silva, and G. R. Satchler, Phys. Letters **4**, 25 (1963).

²⁷ M. Bouten and P. van Leuven, Nucl. Phys. **32**, 499 (1962).

The Hauser-Feshbach calculations for the 1097- and 1189-keV levels in cobalt, gave the results presented by the solid curves on Fig. 5(b). The agreement is reasonable.

The three most abundant isotopes of Zn, comprising more than 95% of natural zinc, have 2^+ excited states at 990, 1040, and 1080 keV. The combined cross sections, for excitation of any of the three levels, are shown on Fig. 5(a). The solid and dashed curves in this figure have the same meaning as above. In this case the measured cross sections strongly favor the Hauser-Feshbach values. This result is difficult to reconcile with current ideas about neutron width distributions. Previous in-

vestigations^{20,22} of Zr⁹⁰ and Fe⁵⁶ have in fact indicated the importance of the width fluctuation for even nuclei.

ACKNOWLEDGMENTS

The authors are indebted to the members of the Applied Nuclear Physics Section for their assistance and to Dr. Peter Moldauer for fruitful discussions. Two of the authors (C. A. Engelbrecht and D. Reitmann) wish to thank the Laboratory Director, Dr. A. V. Crewe, for the hospitality enjoyed at Argonne National Laboratory and also the South African Atomic Energy Board for the opportunity to carry out this work during their overseas tours of duty.

Fe⁵⁴(*d,p*)Fe⁵⁵ Reaction and the Nuclear Structure of Ti⁵¹, Cr⁵³, and Fe⁵⁵†

JAMES R. MAXWELL* AND W. C. PARKINSON

Department of Physics, Cyclotron Laboratory, The University of Michigan, Ann Arbor, Michigan

(Received 17 February 1964)

Energy levels in Fe⁵⁵ have been investigated by means of the Fe⁵⁴(*d,p*)Fe⁵⁵ reaction using 7.8-MeV deuterons from The University of Michigan 42-in. cyclotron. Twenty-eight levels were found up to 5.4 MeV of excitation and angular distributions obtained for eighteen of them. The ℓ_n values and reduced widths were extracted from the data by means of a distorted-wave Born-approximation analysis. An attempt is made to understand the spectra of the 29-neutron nuclei Ti⁵¹, Cr⁵³, and Fe⁵⁵ in terms of a shell-model description involving configurations of 2, 4, or 6 ($1f_{7/2}$) protons and a single neutron in the $2p_{3/2}$, $2p_{1/2}$, or $1f_{5/2}$ orbit.

I. INTRODUCTION

THE nuclei Ti⁵¹, Cr⁵³, and Fe⁵⁵ form an interesting series because each has 29 neutrons with the last neutron and 2, 4, or 6 protons, respectively, outside of a closed-shell core having the structure of the nucleus Ca⁴⁸. The interest arises because the spectrum of Ca⁴⁹ as observed in the (*d,p*) reaction appears to be a pure single-particle spectrum with only three energy levels below an excitation of 3.6 MeV, corresponding to the capture of the neutron into a pure $2p_{3/2}$, $2p_{1/2}$, or $1f_{5/2}$ orbit.¹ In contrast to the situation in Ca⁴⁹, the spectra of Ti⁵¹, Cr⁵³, and Fe⁵⁵ are more complex, there being from six to eight odd parity levels below 4 MeV.²⁻⁸

This paper concerns the properties of energy levels in Fe⁵⁵ which have been studied experimentally by means of the Fe⁵⁴(*d,p*)Fe⁵⁵ reaction and the nuclear structure of Ti⁵¹, Cr⁵³, and Fe⁵⁵.

Thin isotopically enriched targets of Fe⁵⁴ were bombarded with 7.8-MeV deuterons from The University of Michigan 42-in. cyclotron and the outgoing protons analyzed with an over-all resolution of 20 keV using a double focusing magnetic spectrometer. Twenty-eight levels were observed up to an excitation of 5.4 MeV in Fe⁵⁵, and angular distributions were obtained for eighteen of them in the angular range 10° to 60° at 5° intervals and at 70° and 80°. The remaining ten levels were all of very low cross section. Excitation energies were measured and ℓ_n values and reduced widths extracted from the data by means of a distorted-wave analysis.

Since the low-lying levels of the even nuclei Ti⁵⁰, Cr⁵², and Fe⁵⁴ are apparently described rather well in terms of the 2, 4, or 6 ($1f_{7/2}$) protons outside of the Ca⁴⁸ core,⁹ it was thought that the level structure of the odd-*A* nuclei might be understood on the basis of a simple shell-model description in which the 29th neutron in the $2p_{3/2}$, $2p_{1/2}$, or $1f_{5/2}$ orbit is coupled to the possible states of 2, 4, or 6 protons in the $1f_{7/2}$ shell. The results of the shell-model calculation for Ti⁵¹, Cr⁵³,

† Supported in part by the U. S. Atomic Energy Commission.

* Present address: School of Physics, University of Minnesota, Minneapolis, Minnesota.

¹ E. Kashy, A. Sperduto, H. A. Enge, and W. W. Buechner, *Bull. Am. Phys. Soc.* **7**, 315 (1962).

² K. Ramavataram, *Bull. Am. Phys. Soc.* **8**, 367 (1963).

³ K. Ramavataram, *Phys. Rev.* **132**, 2255 (1963).

⁴ J. Bardwick, R. S. Tickle, and W. C. Parkinson, *Bull. Am. Phys. Soc.* **8**, 366 (1963).

⁵ J. Bardwick, Ph.D. thesis, The University of Michigan, 1964 (to be published).

⁶ P. T. Andrews, R. W. Clift, L. L. Green, and J. F. Sharpey-Schafer, University of Liverpool Report, 1963 (unpublished).

⁷ A. Sperduto and J. Rapaport, Massachusetts Institute of Technology Laboratory for Nuclear Science Progress Report, 1961 (unpublished).

⁸ R. H. Fulmer and A. L. McCarthy, *Phys. Rev.* **131**, 2133 (1963).

⁹ I. Talmi, *Phys. Rev.* **126**, 1096 (1962).